Int. J. Heat Mass Transfer. Vol. 28, No. 4, pp. 851–858, 1985
Printed in Great Britain

0017–9310/85 $3.00 + 0.00

Laminar flow through a porous channel bounded by isothermal parallel plates

M. KAVIANY

Department of Mechanical Engineering, University of Wisconsin—Milwaukee, Milwaukee, WI 53201, U.S.A.

(*Received* 28 *June* 1984 *and in final form* 22 *October* 1984)

Abstract—Laminar flow through a porous channel bounded by two parallel plates maintained at a constant and equal temperature is considered. The modified Darcy model for transport of momentum is applied but the velocity square term in the momentum equation and the axial conduction term in the energy equation are neglected. The results show that the Nusselt number for fully-developed fields increases with an increase in the porous media shape parameter, $\gamma = (W^2\varepsilon/K)^{1/2}$, where W is channel width, ε is porosity and K is permeability. The results also show that excess pressure drop, associated with the entrance region, decreases as γ increases.

1. INTRODUCTION

IN CHANNEL flow, enhancement of heat transfer by the insertion of solid matrices has been analyzed [1, 2] and studied experimentally [3] for relatively low permeabilities. In treating these flows, uniform velocity is generally assumed across the channel. However, for relatively high porosities and permeabilities (which are desirable for pressure drop consideration), a non-uniform velocity distribution is expected near the wall. This affects the heat transfer rate from or to the walls. In this study the velocity profile and Nusselt number are determined for flow through a porous channel for a simplified case where the axial conduction in the energy equation and velocity square term in the momentum equation are negligible.

Recent studies in momentum transport through porous media have led to the inclusion of the boundary and the inertia effects for certain flow situations. The boundary effect can be included by adding the viscous shear stress term (due to Brinkman, cf. [4]) or, in cases of media with nonuniform porosity distributions near the bounding rigid surfaces, through modified boundary conditions [4]. Inclusion of the inertia effects is achieved through the so-called non-Darcy term which is proportional to the square of velocity [5] and, also, through the convective term [6]. The results based on inclusion of boundary and inertia effects [6] show that for a boundary-layer flow over a flat plate with free stream velocity $\bar{u}$, fluid viscosity ν, in a porous medium of porosity ε, and permeability K:

(a) the velocity field develops in a short distance from the entrance at a distance of the order of $K\bar{u}\nu^{-1}$, in contrast to an ever developing velocity field where no rigid matrix is present;

(b) the momentum boundary-layer thickness is of the order of $(K/\varepsilon)^{1/2}$; and

(c) at high Prandtl numbers, the inclusion of boundary effects alters the rate of heat transfer from the surface significantly.

Similar results are expected for flow through a porous medium bounded by the parallel planes maintained at equal and constant temperatures (shown schematically in Fig. 1). In this case both the velocity and temperature fields will eventually become fully developed. By including the boundary effect, the boundary friction

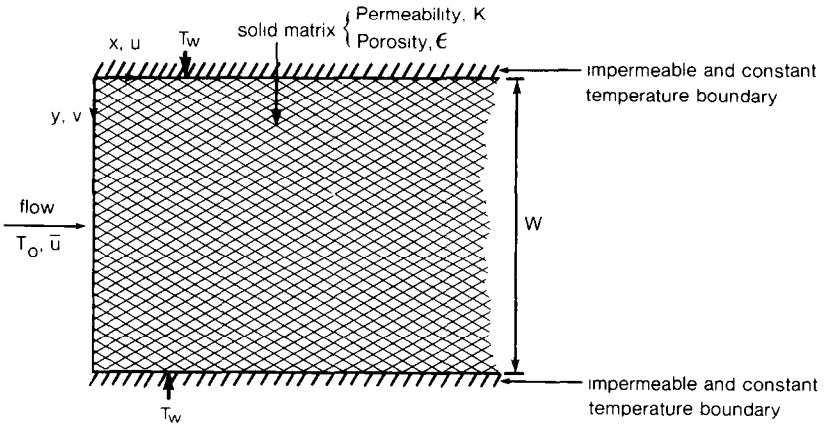

FIG. 1. Schematic of the problem considered.

NOMENCLATURE

c_p	specific heat at constant pressure
F	the empirical coefficient given in ref. [6]
f	boundary frictional drag coefficient, $2\tau_w/(\rho_f \bar{u}^2)$
k_e	effective thermal conductivity
K	permeability of porous medium
Nu	Nusselt number for fully-developed fields, $q_w 2W(T_w-\bar{T})^{-1}k_e^{-1}$
p	pressure
Pe'	Peclet number, $2\bar{u}W\alpha_e^{-1}$
Pr	Prandtl number, ν_f/α_e
q_w	wall heat flux
Re	Reynolds number, $2\bar{u}W\nu_f^{-1}$
T	temperature, $(T-T_w)/(T_0-T_w)$
$\bar{T}$	mean temperature, $(W\bar{u})^{-1}\int_0^W uT\,dy$
u	x-direction velocity
$\mathbf{u}$	velocity vector
$\bar{u}$	mean x-direction velocity, over $0 \leqslant y \leqslant W$
v	y-direction velocity
W	width of the channel
x, y	spatial coordinates, parallel and perpendicular to the direction of flow, respectively.

Greek symbols

α_e	effective thermal diffusivity, $(\rho C_p)_f^{-1}\varepsilon^{-1}k_e$
γ	porous media shape parameter, $(W^2\varepsilon/K)^{1/2}$
ε	porosity
μ	dynamic viscosity
ν	kinematic viscosity
ρ	density
τ_w	wall shear stress, $2\rho_f\nu_f u_y\,(y=0)$
Φ	excess pressure drop.

Subscripts

D	associated with Darcy's analysis
f	fluid
o	entrance condition
max	maximum value
s	solid matrix
T	total
w	wall condition
x, y	x, y-derivative.

Others

$\langle\ \rangle$	local value average, for a scalar ψ, $\langle\psi\rangle = v^{-1}\int v_f\psi\,dv$.

drag and the average Nusselt number for fully-developed fields can be determined. Also, by including the convective term in the momentum equation, the development of the velocity field as indicated by the excess pressure drop and the entrance length is examined.

There are two natural length scales associated with the problem considered. One is the pore–particle dimension which is $(K/\varepsilon)^{1/2}$ and the other the channel width, W. The latter is chosen here as the characteristic length; but, as will be shown, through the porous media shape parameter, the small scale boundary effects such as the thickness of the boundary layer can still be determined.

This study is limited to situations in which (i) fluid and solid phases are in local thermal equilibrium; (ii) the velocity square term in the momentum equation is negligible; and (iii) the axial conduction term in the energy equation is negligible. These are idealizations that may not be completely realized simultaneously. However, the results obtained here, especially those for fully-developed fields, are expected to be valid even if the limits are slightly relaxed.

2. GOVERNING EQUATIONS

It is assumed that the fluid and the solid matrix are in local thermal equilibrium and that the magnitudes of the thermophysical properties are constant. Under these assumptions and by treating the solid matrix and the fluid as a continuum, the governing differential equations are given in [6] for uniform porosity distribution are

$$\nabla\cdot\langle u\rangle = 0, \tag{1}$$

$$\varepsilon^{-1}\rho_f\langle(\mathbf{u}\cdot\nabla)\mathbf{u}\rangle = -\varepsilon^{-1}\nabla\langle p\rangle + \varepsilon^{-1}\mu_f\nabla^2\langle\mathbf{u}\rangle - K^{-1}\mu_f\langle\mathbf{u}\rangle - F\varepsilon K^{-1/2}\rho_f(\langle\mathbf{u}\rangle\cdot\langle\mathbf{u}\rangle)\mathbf{l} \tag{2}$$

$$(\langle\mathbf{u}\rangle\cdot\nabla)\langle T\rangle = \alpha_e\nabla^2\langle T\rangle, \tag{3}$$

where $\mathbf{l}$ is the pore velocity unit vector. For a two-dimensional flow, the following equations emerge when the volume average symbol is dropped and the variables are nondimensionalized with respect to W, $\bar{u}$, T_o-T_w, and $\rho_f\bar{u}^2$ as the scales for length, velocity, temperature and pressure, respectively.

$$u_x + v_y = 0 \tag{4}$$

$$uu_x + vu_y = -P_x + 2\,Re^{-1}(u_{xx}+u_{yy}) - 2\,Re^{-1}\gamma^2 u - F\varepsilon^{3/2}\gamma(\mathbf{u}\cdot\mathbf{u})\mathbf{l}\cdot\mathbf{i} \tag{5}$$

$$uv_x + vv_y = -P_y + 2\,Re^{-1}(v_{xx}+v_{yy}) - 2\,Re^{-1}\gamma^2 v - F\varepsilon^{3/2}\gamma(\mathbf{u}\cdot\mathbf{u})\mathbf{l}\cdot\mathbf{i} \tag{6}$$

$$uT_x + vT_y = 2\,Pe'^{-1}T_{xx} + 2\,Pe'^{-1}T_{yy}. \tag{7}$$

Here $\langle(\mathbf{u}\cdot\nabla)\mathbf{u}\rangle$ is approximated as $(\langle\mathbf{u}\rangle\cdot\nabla)\langle\mathbf{u}\rangle$. The porous media shape parameter, γ, is equal to $(W^2\varepsilon/K)^{1/2}$ and is the ratio of the large to small length scales.

The quantities are averaged over the local volume of the fluid plus the local volume of the solid matrix. In the entrance problem considered, the velocity field specified at the entrance is that associated with the porous medium, not with the medium preceding it.

The boundary conditions used are:

Entrance:

$$x = 0, \quad v = 0, \quad u = 1, \quad p = p_o, \quad T = 1 \tag{8}$$

Solid Boundaries:

$$y = 0, 1, \quad u = 0, \quad v = 0, \quad T = 0 \tag{9}$$

Exit:

$$\text{for fully-developed flow } v = 0, \quad u = u(y) \text{ only.} \tag{10}$$

Far from the entrance the temperature of the medium will be the same as that of the walls. However, for any finite length and fully-developed fields, an invariant temperature distribution and an invariant local Nusselt number exist [18]. The heat transfer results are given in terms of the Nusselt number for fully-developed flow, i.e.

$$Nu = -2T_y(y = 0)(T_w - \bar{T})^{-1}. \tag{11}$$

The system has a symmetry axis that passes through $y = 0.5$. The integration of equations (1)–(3) is done numerically for the developing flow situation and in closed analytical form for the fully-developed flow situation. The numerical results are obtained via finite-difference approximation using a combination of pressure correction techniques, the power law approximation, and the staggered grid system as recommended by Patankar [7].

For validation of the numerical integration, the results for the case of $\gamma = 0$ were compared against the results available in the literature [8–18]. The numerical integration scheme was also validated by comparison with the closed form solutions obtained here. In all cases complete agreement has been found.

3. FULLY-DEVELOPED FIELDS FOR A SIMPLIFIED CASE

3.1. *Hydrodynamic aspects*

In the case of a fully-developed flow, equation (5) becomes

$$u_{yy} - \gamma^2 u - \tfrac{1}{2}F\varepsilon^{3/2}\gamma u^2 = \tfrac{1}{2}Re\, p_x, \quad \text{where } p_x = \text{constant.} \tag{12}$$

In order to obtain a simple closed form solution to this equation, the $\frac{1}{2}F\varepsilon^{3/2}\gamma u^2$ term will be omitted. The conditions under which this is allowable are given in [6]. Then, the closed form solution to equation (12) subject to the boundary conditions given by equation (9) is

$$u = [1 - e^{-2\gamma} - (1 - e^{-\gamma})(e^{\gamma(y-1)} + e^{-\gamma y})] \times [1 - e^{-2\gamma} - 2(1 - e^{-\gamma})^2\gamma^{-1}]^{-1}. \tag{13}$$

Equation (13) was obtained by first determining the velocity profile from the dimensional form of equation (12) and then evaluating the average velocity and, finally, dividing the former by the latter. The maximum velocity (normalized with respect to the mean velocity) which takes place at the mid-distance between the two plates is

$$u_{max} = [1 - e^{-2\gamma} - 2(1 - e^{-\gamma})\, e^{-\gamma/2}] \times [1 - e^{-2\gamma} - 2(1 - e^{-\gamma})^2\gamma^{-1}]^{-1}. \tag{14}$$

For large γ, this becomes:

$$u_{max} \simeq \gamma(\gamma - 2)^{-1}, \quad \gamma > 20. \tag{15}$$

The dimensionless boundary frictional drag can now be evaluated and the result is

$$f = 8\gamma\, Re^{-1}(1 - e^{-\gamma})^2[1 - e^{-2\gamma} - 2(1 - e^{-\gamma})^2\gamma^{-1}]^{-1}. \tag{16}$$

As expected, when $\gamma \to 0$ this becomes

$$f = 48\, Re^{-1}, \quad \text{as } \gamma \to 0. \tag{17}$$

In addition to the boundary frictional drag, the fully-developed flow through a porous medium also experiences a bulk frictional drag induced by the solid matrix (designated as Darcy's pressure drop) which in dimensionless form is

$$\Delta p_D = 2\gamma^2\, Re^{-1}x. \tag{18}$$

Now, by adding the excess pressure loss $\Phi(x)$, which takes place at the entrance region, to these two pressure losses, the total pressure loss for the developing flow in the porous medium is

$$\Delta p_T(x) = 2\gamma^2\, Re^{-1}x + 4\gamma\, Re^{-1}(1 - e^{-\gamma})^2 \times [1 - e^{-2\gamma} - 2(1 - e^{-\gamma})^2\gamma^{-1}]^{-1}x + \Phi(x). \tag{19}$$

Note that the friction factor is the shear stress at the walls divided by $(1/2)\rho_f \bar{u}^2$ while the pressure is nondimensionalized using $\rho_f \bar{u}^2$. As will be shown, Φ is negligibly small compared to the first and second terms in equation (19). The following limits hold:

$$f \simeq 8\gamma\, Re^{-1}, \quad \gamma > 100, \tag{20}$$

and since the bulk drag is proportional to γ^2 while the boundary drag is proportional to γ, we have

$$\Delta p_T \simeq 2\gamma^2\, Re^{-1}x, \quad \gamma > 200. \tag{21}$$

3.2. *Heat transfer aspects*

In the case of a fully-developed velocity field, equation (7) becomes

$$uT_x = 2Pe'^{-1}T_{xx} + 2Pe'^{-1}T_{yy}. \tag{22}$$

In order to simplify the analysis and also to make it possible to compare the results with those available in

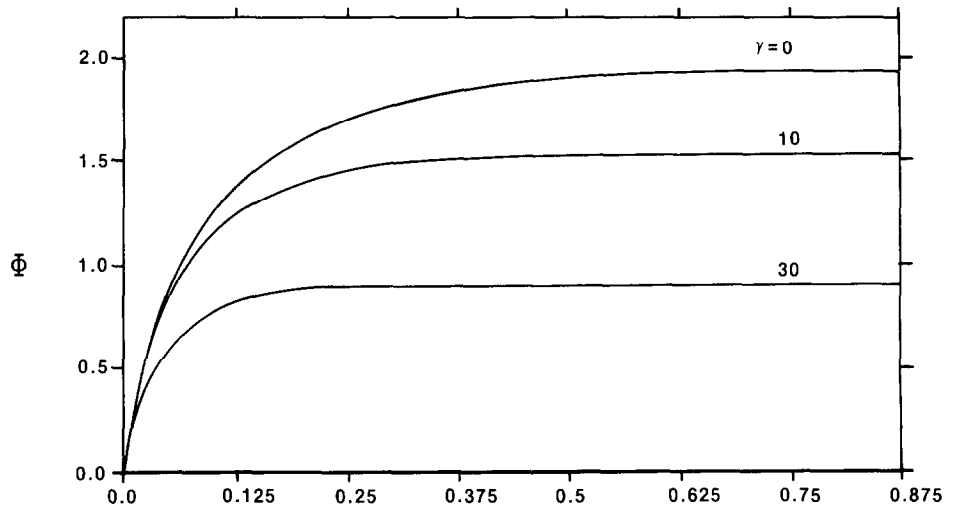

FIG. 2. Excess pressure drop distribution for several values of the porous media shape parameter. Reynolds number is 10.

the literature for $\gamma = 0$, the axial conduction term will be neglected. In equation (22) u is given by equation (13) and the boundary conditions for temperature are those given by equations (8) and (9). The criterion for the thermally fully-developed flow is that the local Nusselt number and the invariant temperature profile no longer change as the axial distance increases. Then, the fully-developed heat transfer results depend on the porous media shape parameter only.

For very large γ the velocity profile given by equation (13) is that of slug flow, i.e. the velocity distribution is uniform. For this limiting case the Nusselt number is 9.87 [19]. Therefore, the Nusselt number of the fully-developed fields varies between 7.54 (for $\gamma = 0$) and 9.87 (for $\gamma \to \infty$) depending on the value of γ. The results, which are obtained by numerical integration, are presented in the next section.

4. RESULTS AND DISCUSSION

4.1. *Hydrodynamic aspects*

The results for the hydrodynamic characteristics are shown in Figs. 2–5. Note that these results are based on the assumption that the contribution from the velocity-square term is negligible. The development region is generally characterized by the excess pressure drop that takes place in this region. This quantity is determined as a function of x from

$$\Phi(x) = \Delta p_T(x) - \Delta p_D(x) - \tfrac{1}{2} f x. \tag{23}$$

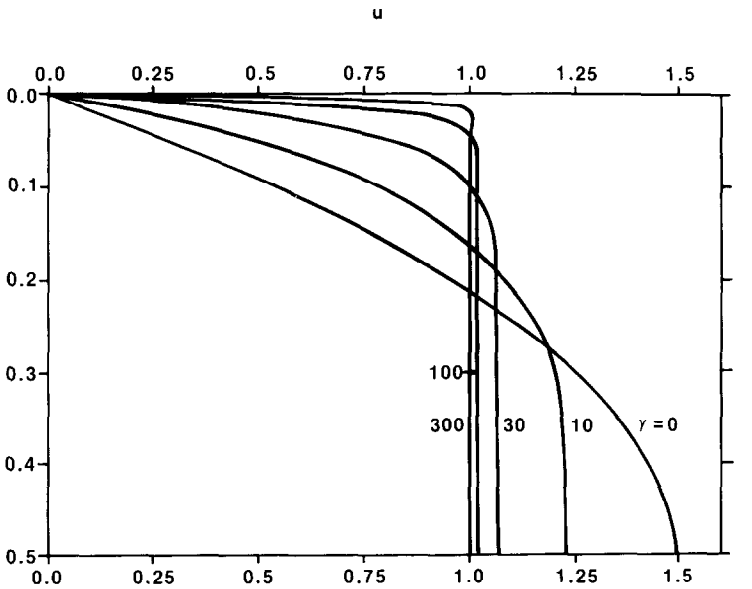

FIG. 3. The fully-developed velocity distribution for several values of the porous media shape parameter.

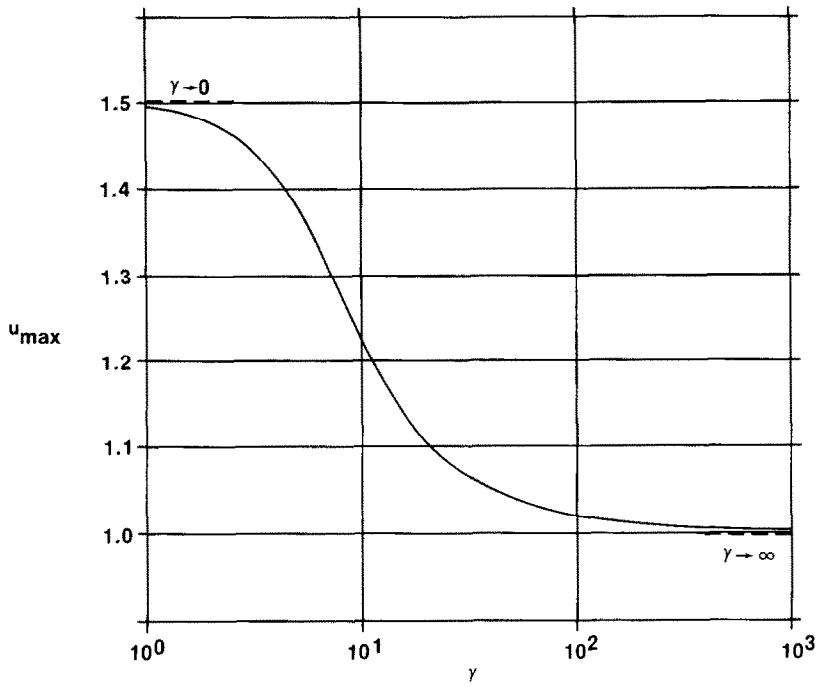

FIG. 4. The magnitude of the maximum (centerline) velocity (as a function of the porous media shape parameter). The limit for $\gamma \to \infty$ is also shown.

The entrance length, i.e. the longitudinal distance at which the center-line velocity is 99% of its value for a fully-developed field, is given in [12] for $\gamma = 0$ by the following approximation:

$$x_e/w = 0.63\,(0.018\,Re+1)^{-1}+0.022\,Re, \quad \text{for} \quad \gamma = 0. \quad (24)$$

In [12] the Reynolds number is based on W rather than $2W$. A similar expression is given for the excess pressure drop [12]. However, as shown in [9], no simple and accurate expressions can be given for the excess pressure drop and entrance length which are valid for all Reynolds numbers. As an example, Fig. 2 shows the effect of the porous media shape parameter on the

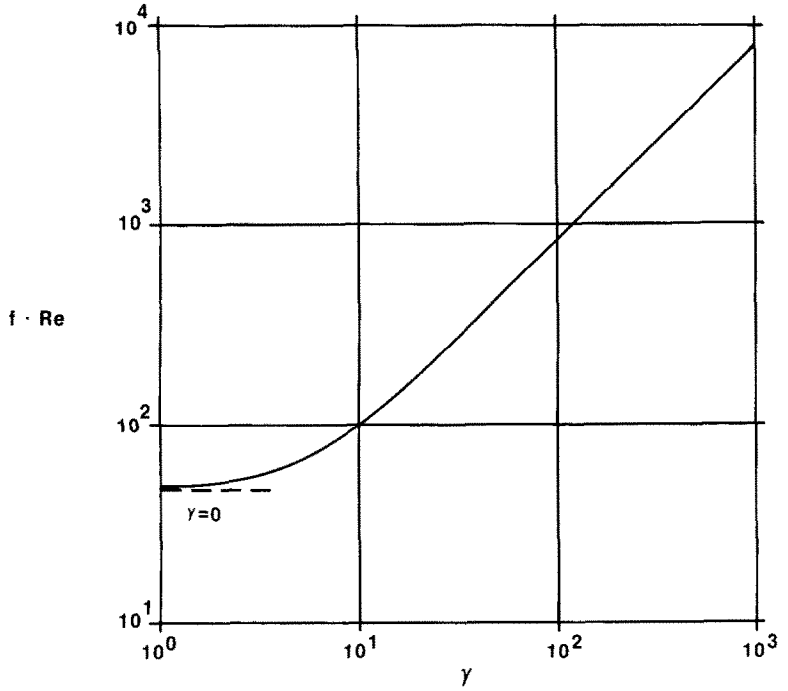

FIG. 5. Variation of the wall friction factor with the porous media shape parameter.

excess pressure drop for $Re = 10$. The results show that the excess pressure drop decreases rather rapidly as γ increases. The results also show that the entrance length decreases rather rapidly as γ increases ($x_e/w = 0.75$ for $\gamma = 0$ and $Re = 10$). This trend is also found in [6] through dimensional analysis, i.e. the entrance length was found to be proportional to γ^{-2}. Therefore, the entrance length for the porous medium is much shorter than that for a nonporous medium and is generally negligible. A similar trend is expected for other Reynolds numbers.

Equation (24) shows that the dimensional entrance length increases with an increase in W for $\gamma = 0$. However, as shown in Fig. 2 if Re, ε and K are kept constant, as W increases, γ increases and the nondimensional entrance length decreases. This is because as the ratio of the large to small-length scales increases, the boundary effects become less significant, i.e. the effect of the no-slip boundary condition does not penetrate as far. Therefore, for $\gamma \neq 0$, the dimensional entrance length does not increase monotonically with W.

As to the relative importance of the excess pressure drop, examination of equation (19) reveals that the entrance pressure drop is important only for small values of γ.

Figure 3 shows the effect of γ on the fully-developed velocity profile which contains a flat portion located around the centerline. This flat portion, which extends further toward the solid surfaces as γ increases, explains the reason for the shorter entrance length as γ increases. The profiles plotted in Fig. 3 are given by equation (13). Note that the boundary-layer thickness decreases as γ increases. This is the trend found in [6] by dimensional analysis which showed that the momentum boundary-layer thickness is of the order of γ^{-1}.

The maximum velocity, which takes place at the centerline, decreases with increases in γ. This trend is shown in Fig. 4. The results are also given by equation (14). The results show that for $\gamma > 10^2$ the magnitude of the centerline velocity is almost unity. This is also evident from equation (15). It should be noted that for large γ the velocity profile is that of a slug flow.

The fully-developed wall friction factor given by equation (16) is also shown in Fig. 5. The results show that as γ approaches zero, fRe^{-1} approaches its value for when no rigid matrix is present as given by equation (17). The results for this total pressure drop can be summarized as:

$$\Delta p_T(x) = 2\gamma^2 Re^{-1}x + 4\gamma Re^{-1}(1-e^{-\gamma})^2 \times [1-e^{-2\gamma}-2(1-e^{-\gamma})^2\gamma^{-1}]^{-1}x + \Phi(x),$$

$$\Delta p_T \simeq 2\gamma^2 Re^{-1}x \quad \text{for} \quad \gamma > 100.$$

4.2. *Heat transfer aspects*

The variation of the Nusselt number for fully-developed temperature and velocity fields as a function of the porous media shape parameter is shown in Fig. 6. The results are independent of Pe' and Pr. The trend is similar to that found for the magnitude of the maximum velocity (Fig. 4), i.e. that for $\gamma > 300$ the magnitude of Nu reaches its asymptotic value of 9.87 for slug flow. As expected, for $\gamma = 0$ the magnitude of Nu is equal to 7.54.

Finally, the temperature distribution for the fully-developed fields (both thermal and hydrodynamic) is shown in Fig. 7. Again, the results are independent of

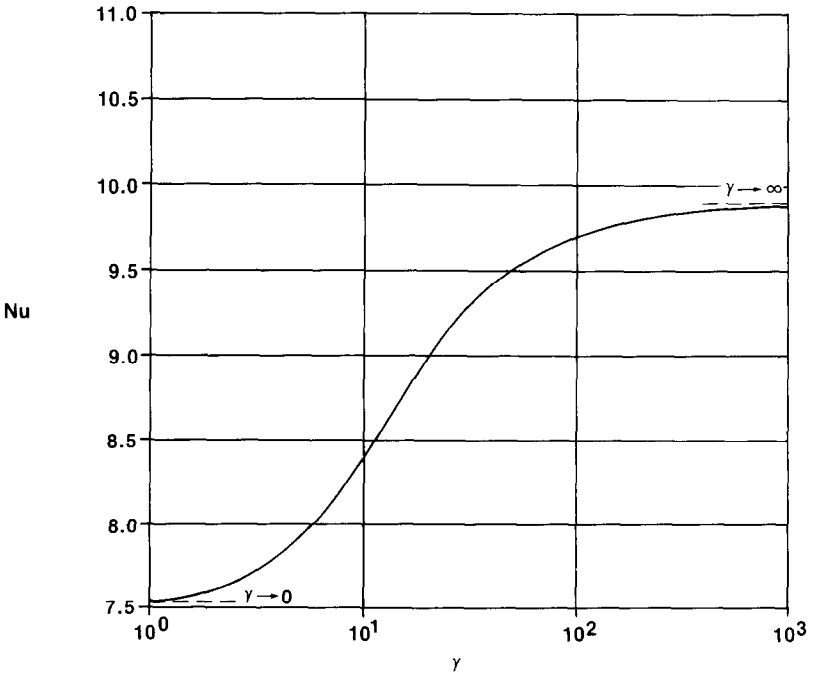

FIG. 6. Variation of the fully-developed local Nusselt number with the porous media shape parameter. The asymptotic value for $\gamma \to \infty$ is also shown.

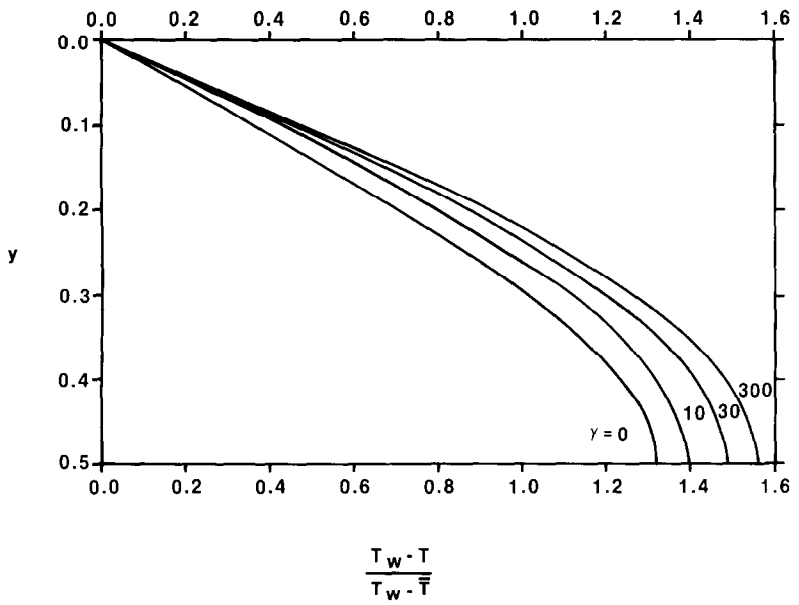

FIG. 7. The invariant fully-developed temperature profiles for several values of the porous media shape parameter.

Pe' and Pr. This distribution is plotted in the conventional form which is an invariant with respect to x for finite channel length and the fully-developed fields. In contrast to the fully-developed velocity profiles, the shape of the profile does not change significantly by the introduction of the solid matrix. The results also show that the centerline temperature increases with increases in γ.

Table 1 gives the values of the porous shape parameter for some relatively high permeability porous inserts, such as foam metals. As can be seen, values of less than 10^3 for γ are obtainable in some small channels with relatively high permeability solid matrices.

By insertion of the solid matrix, the heat transfer rate from or to the walls, given by $Nuk_e(T_w - \bar{T})(2W)^{-1}$, increases through increases in Nu and k_e.

In [1] an allowance was made for the temperature difference between the solid and fluid phases, i.e. two-phase model. As the interstitial heat transfer coefficient becomes relatively large, this temperature difference becomes negligible, as was assumed here.

Table 1. The values of porous media shape parameters for some high permeability porous inserts

W (m)	ε	K (m^2)	γ
10^{-1}	0.9	10^{-5}	3×10^1
		10^{-7}	3×10^2
		10^{-9}	3×10^3
10^{-2}		10^{-7}	3×10^1
		10^{-9}	3×10^2
		10^{-11}	3×10^3

5. SUMMARY

The governing equations, which assume local thermal equilibrium between the solid matrix and the fluid and include the convective and boundary effects, are solved for developing flows between parallel plates where the axial conduction and velocity-square terms are neglected. As a result, the following are determined.

5.1. *Hydrodynamic characteristics*

(a) The excess pressure drop experienced in the entrance region decreases with increases in the porous media shape parameter γ, and for large values of γ it is negligible compared to the boundary friction drag and bulk frictional drag induced by the solid matrix.

(b) The hydrodynamic entrance length decreases rapidly with an increase in γ. This is as was predicted by others [6] for flow over a plate in saturated porous media.

(c) The fully-developed velocity profile depends strongly on γ. As γ increases, the central region containing a uniform velocity distribution spreads further toward the plates. At large γ, the velocity variation is confined to a very thin layer adjacent to the plates.

(d) The magnitude of the centerline velocity decreases with γ. This variation is most significant for $3 < \gamma < 50$.

(e) The boundary frictional drag coefficient is proportional to γ while the bulk frictional drag coefficient is proportional to γ^2. As a result, for γ larger than 200 the boundary friction loss can be neglected compared to the bulk friction loss.

5.2. *Heat transfer characteristics*

(a) The distribution of the local Nusselt number in the

entry region has the same Prandtl number dependency as that for a nonporous medium. The combined entrance length decreases with an increase in γ and also decreases with a decrease in Prandtl number.

(b) The fully-developed Nusselt number increases with an increase in γ, and its value is sensitive to the magnitude of γ for $1 < \gamma < 10^3$. Below this limit the Nusselt number is 7.54 and above this limit the Nusselt number is 9.87.

(c) While the shape of the invariant temperature profile for the fully-developed fields does not change significantly with γ, its value at the centerline increases as γ increases.

REFERENCES

1. J. C. Y. Koh and R. Colony, Analysis of cooling effectiveness for porous material in a coolant passage, *J. Heat Transfer* **96,** 324–330 (1974).
2. K. Y. Wang and C. L. Tien, Thermal insulation in flow systems: combined radiation and convection through a porous segment, *J. Heat Transfer* **106,** 453–459 (1984).
3. J. C. Y. Koh and R. L. Stevens, Enhancement of cooling effectiveness by porous materials in coolant passages, *J. Heat Transfer* **97,** 309–311 (1975).
4. D. A. Nield, The boundary condition for the Rayleigh–Darcy problem: limitation of the Brinkman equation, *J. Fluid Mech.* **128,** 37–40 (1983).
5. C. S. Beaver and E. M. Sparrow, Non-Darcy flow through porous media, *J. appl. Mech.* **36,** 711–714 (1969).
6. K. Vafai and C. L. Tien, Boundary and inertia effects on flow and heat transfer in porous media, *Int. J. Heat Transfer* **24,** 195–203 (1981).
7. S. V. Patankar, *Numerical Heat Transfer and Fluid Flow.* Hemisphere, New York (1980).
8. Y. L. Wang and P. A. Longwell, Laminar flow in the inlet section of parallel plates, *A.I.Ch.E. Jl* **10,** 323–329 (1964).
9. F. W. Schmidt and B. Zeldin, Laminar flow in inlet section of tubes and ducts, *A.I.Ch.E. Jl* **15,** 612–614 (1969).
10. H. S. Lew and Y. C. Fung, Entry flow into blood vessels at arbitrary Reynolds numbers, *J. Biomech.* **3,** 23–38 (1970).
11. B. Atkinson, M. P. Brockleband, C. C. H. Card and J. M. Smith, Low Reynolds number developing flows, *A.I.Ch.E. Jl* **15,** 548–553 (1969).
12. R.-Y. Chen, Flow in the entrance region at low Reynolds numbers, *J. Fluid Engng* **95,** 153–158 (1973).
13. H. S. Lew and J. Miller, A low Reynolds number entry flow theory and its application to the motion of the plasma in blood flows, *J. Biomech.* **7,** 113–121 (1974).
14. B. S. Narang and G. Krishnamurthy, Laminar flow in the entrance region of parallel plates, *J. appl. Mech.* **43,** 186–188 (1976).
15. S. C. R. Dennis, A. McD. Mercer and G. Poots, Forced heat convection in laminar flow through rectangular ducts, *Quant. appl. Math.* **17,** 285–297 (1959).
16. H. S. Heaton, W. C. Reynolds and W. M. Kays, Heat transfer in annular passages. Simultaneous development of velocity and temperature fields in laminar flow, *Int. J. Heat Mass Transfer* **7,** 763–781 (1964).
17. R. K Shah and A. C. London, Thermal boundary conditions and some solutions for laminar duct flow forced convection, *J. Heat Transfer* **96,** 159–165 (1974).
18. W. M. Kays and M. E. Crawford, *Convective Heat and Mass Transfer.* McGraw-Hill, New York (1980).
19. W. Rohsenow and J. Hartnett (editors), *Handbook of Heat Transfer,* p. 124. McGraw-Hill, New York (1973).

ECOULEMENT LAMINAIRE A TRAVERS UN CANAL POREUX LIMITE PAR DES PLANS PARALLELES ISOTHERMES

Résumé—On considère un écoulement laminaire à travers un canal poreux limité par deux plans parallèles maintenus à une température identique et uniforme. Le modèle de Darcy modifié pour le transport de quantité de mouvement est appliqué mais on néglige le terme du carré de la vitesse dans l'équation de quantité de mouvement et le terme de conduction axiale dans l'équation d'énergie. Ces résultats montrent que le nombre de Nusselt, pour les champs pleinement établis, augmentent avec le paramètre de forme du milieu poreux $\tau = (W^2\varepsilon/K)^{1/2}$, où W est la largeur du canal, ε la porosité et K la perméabilité. Les résultats montrent aussi que l'excès de chute de pression, associé à la région d'entrée, décroît lorsque γ augmente.

LAMINARE STRÖMUNG DURCH EINEN PORÖSEN KANAL, DER DURCH ISOTHERME PARALLELE PLATTEN BEGRENZT IST

Zusammenfassung—Es wird eine laminare Strömung durch einen porösen Kanal, der durch zwei parallele Platten gleicher konstanter Temperatur begrenzt ist, betrachtet. Das modifizierte Darcy-Modell für den Impulstransport wird verwendet, wobei jedoch der quadratische Geschwindigkeitsterm in der Impulsgleichung und der axiale Leitungsterm in der Energiegleichung vernachlässigt werden. Die Ergebnisse zeigen, daß die Nusselt-Zahl im voll ausgebildeten Zustand ansteigt, wenn der Formparameter des porösen Mediums $\gamma = (W^2\varepsilon/K)^{1/2}$ ansteigt; dabei bedeutet W die Kanalbreite, ε die Porosität und K die Permeabilität. Die Ergebnisse zeigen auch, daß der zusätzliche Druckabfall im Eintrittsbereich mit steigenden γ abnimmt.

ЛАМИНАРНОЕ ТЕЧЕНИЕ ЧЕРЕЗ ПОРИСТЫЙ КАНАЛ, ОГРАНИЧЕННЫЙ ИЗОТЕРМИЧЕСКИМИ ПАРАЛЛЕЛЬНЫМИ ПЛАСТИНАМИ

Аннотация—Рассматривается ламинарное течение через пористый канал, ограниченный двумя параллельными пластинами, поддерживаемыми при постоянных равных температурах. Применяется модифицированная модель Дарси для переноса количества импульса, при этом квадратичный по скорости член в уравнении сохранения импульса и аксиальная теплопроводность в уравнении энергии считаются пренебрежимо малыми. Результаты показывают, что число Нуссельта для полностью развитых течений увеличивается с ростом параметра формы пористой среды, $\gamma = (W^2\varepsilon/K)^{1/2}$, где W—ширина канала, ε— пористость и K– проницаемость. Из результатов также видно, что добавочный перепад давления на входном участке растет с увеличением γ.